Oral presentation | Incompressible/compressible/hypersonic flow

Incompressible/compressible/hypersonic flow-IV

Thu. Jul 18, 2024 2:00 PM - 4:00 PM Room D

[11-D-02] Novel implicit finite volume frameworks for hypersonic steady flow problems.

*Benoît Cossart[1,2], Raphaël Loubère[2], Jean-Philippe Braeunig[1] （1. CEA-CESTA, 2. Université de Bordeaux）

Keywords: Hypersonic steady flow, Finite-Volume, Implicit scheme, Euler Equations

Novel implicit finite volume framework for hypersonic steady state flows

ICCFD 12, 15 to 19th July 2024

B. Cossart [1,2] (benoit.cossart@u-bordeaux.fr)
R. Loubère [2] (raphael.loubere@u-bordeaux.fr)
JP. Braeunig [1] (jean-philippe.braeunig@cea.fr)
[1] CEA-CESTA [2] Institut mathématiques de Bordeaux

Motivation and objective:

introduction

Physical context:
Atmospheric re-entry, an highly multi-physics problem:

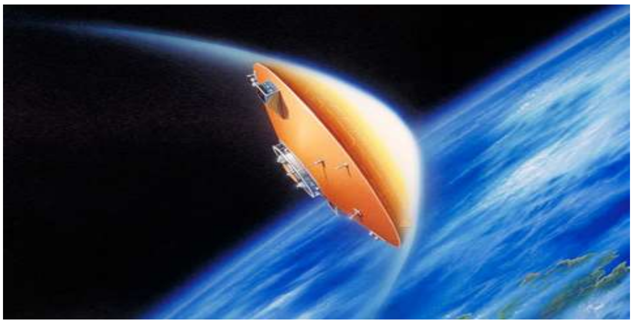

Hypersonic flow, strong heat transfer, turbulence, chemical reactions, ablation, shock waves...

Numerical context:
Flows around various shapes, quasi-steady flows statement [1]:

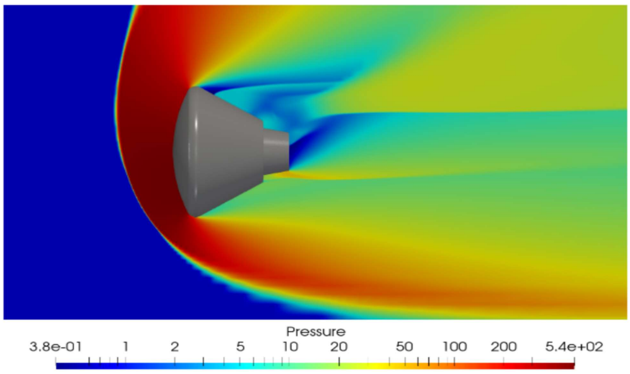

Implicit numerical linearized Finite Volumes (FV) method. First, multi-D Euler's equations.

Nowadays: Classical [8] methods. ad-hoc CFL ramping is mandatory.

Motivation and objective:

A symptomatic case: 1D Burgers' equation

Implicit method with classical Yee linearization procedure must be used with ad-hoc CFL ramping to ensure stability. Illustration on simple 1D Burgers' equation over 100 points uniform mesh.

Continuous model:

Burgers' equation: $\partial_t u + \partial_x f(u) = 0$

with, $f(u) = \frac{u^2}{2}$

Numerical result:

Anomaly when $CFL > 1$

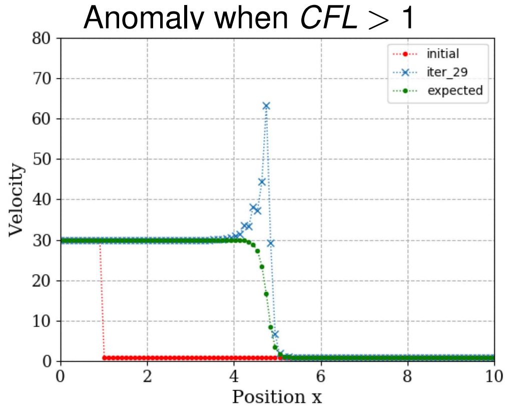

Initial profile:

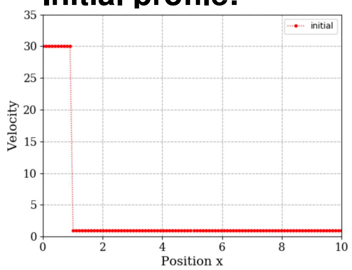

CFL ramping:

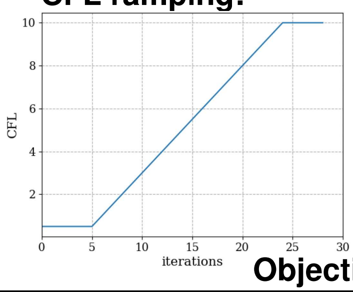

Objective:

Propose theoretical tools to analyse existing methods, and also design novel, more robust, more efficient, and well suited ones for 2D/3D unstructured meshes.

Outline

Analysis of multi-D Euler equations linearization procedure

- Euler equations: physical & numerical model
- Stability analysis
- Numerical results

Linear stability analysis

- Generic linearization for implicit schemes
- A novel matrix correction
- Numerical results

A new paradigm: flux re-formulation of Euler equations

Analysis of multi-D Euler equations linearization procedure

Euler equations: physical & numerical model

Continuous model:

system of PDEs: $\partial_t \mathbf{U} + \nabla \cdot \mathbf{F} = 0$

Discretized model:

$$\frac{\mathbf{U}_c^{n+1} - \mathbf{U}_c^n}{\Delta t} + \sum_f S_f \mathbf{\Phi}_f^{n+1} . \mathbf{n}_{cf} = 0$$

FV-Roe Riemann solver [6]...
to work with the hyperbolic structure of the system

$$\mathbf{\Phi}_f^{n+1} = \frac{\mathbf{F}_d^{n+1} + \mathbf{F}_c^{n+1}}{2} . \mathbf{n}_{cf} - |\mathbb{J}_f^n|_\varepsilon \left(\frac{\mathbf{U}_d^{n+1} - \mathbf{U}_c^{n+1}}{2} \right)$$

... with Harten entropy fix [5]...

$$|\lambda_c|_\varepsilon = \begin{cases} |\lambda_c| & \text{if } |\lambda_c| \geq 2\varepsilon \\ \frac{\lambda_c^2}{4\varepsilon} + \varepsilon & \text{if } |\lambda_c| < 2\varepsilon \end{cases}$$

... and carbuncle filtering

Application on unstructured meshes

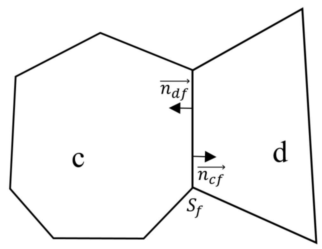

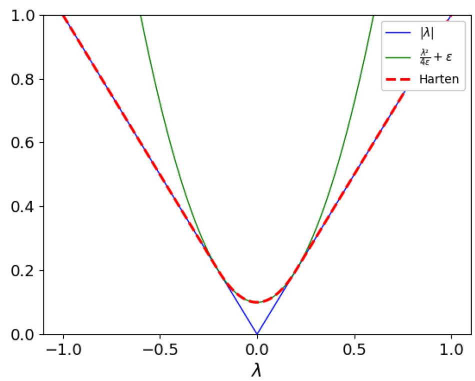

blue, absolute value
red, smoothed absolute value

-

Analysis of multi-D Euler equations linearization procedure

Euler equations: physical & numerical model

Discretized model:

$$\frac{\mathbf{U}_c^{n+1} - \mathbf{U}_c^n}{\Delta t} + \sum_f S_f \boldsymbol{\Phi}_f^{n+1}(\mathbf{n}_{cf}) = 0$$

Increment linearization : $\boldsymbol{\Phi}_f^{n+1} = \boldsymbol{\Phi}_f^n + \Delta\boldsymbol{\Phi}_f$

Classical [8] linearization:

Using $\Delta\mathbf{F}_c \approx \mathbb{J}_c^n \Delta\mathbf{U}_c$

$$\Delta\boldsymbol{\Phi}_f \approx \frac{\mathbb{J}_c^n \Delta\mathbf{U}_c + \mathbb{J}_d^n \Delta\mathbf{U}_d}{2} - |\mathbb{J}_f^n| \frac{\Delta\mathbf{U}_d - \Delta\mathbf{U}_c}{2}$$

Generic implicit scheme:

$\Delta\mathbf{U} = \mathbf{U}^{n+1} - \mathbf{U}^n$

$$\boxed{\underbrace{\left(\frac{\mathbb{I}}{\Delta t} + \sum_f S_f \mathbb{A}_{cf}\right)\Delta\mathbf{U}_c - \sum_f S_f \mathbb{A}_{df} \Delta\mathbf{U}_d = \sum_f S_f \Phi_f^n(\mathbf{n}_{cf})}_{\mathbb{A}\Delta\mathbf{U} = \mathbf{B}}}$$

Block matrices:

$$\mathbb{A}_{cf} = \frac{|\mathbb{J}_f| - \mathbb{J}_c}{2} \quad \& \quad \mathbb{A}_{df} = \frac{|\mathbb{J}_f| - \mathbb{J}_d}{2}$$

Analysis of multi-D Euler equations linearization procedure

Stability analysis

1D system von Neumann type linear analysis on each component α with assumptions

1D generic implicit structure:

$$-(\mathbb{A}_{i+1}\Delta\mathbf{U}_{i+1})_\alpha + \frac{(\Delta\mathbf{U}_i)_\alpha}{\tau} + (\mathbb{A}_i\Delta\mathbf{U}_i)_\alpha - (\mathbb{A}_{i-1}\Delta\mathbf{U}_{i-1})_\alpha = -\left(\mathbf{\Phi}^n_{i+1/2} - \mathbf{\Phi}^n_{i-1/2}\right)_\alpha$$

Hypothesis:

- $\mathbb{A}_i$ & $\mathbb{A}_{i\pm1}$ frozen at t^n
- Using $\mathbf{F}_i = \mathbb{J}_i\mathbf{U}_i$ for Euler equations
- $\left(\mathbb{A}_i\widehat{\mathbf{U}}^{n+1}_i\right)_\alpha \simeq \theta_\alpha\left(\mathbb{A}_i\widehat{\mathbf{U}}^n_i\right)_\alpha$

$$\left(\widehat{\mathbf{U}}^{n+1}_i\right)_\alpha = \theta_\alpha\left(\widehat{\mathbf{U}}^n_i\right)_\alpha$$
$$\widehat{\mathbf{U}}^n_{i\pm1} = e^{\pm jk\Delta x}\widehat{\mathbf{U}}^n_i$$

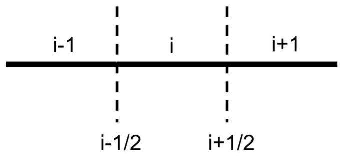

$$\theta_\alpha = \frac{\frac{1}{\tau}}{\frac{1}{\tau} + \frac{\left((\mathbb{A}_i - \mathbb{A}_{i+1}e^{jk\Delta x} - \mathbb{A}_{i-1}e^{-jk\Delta x})\widehat{\mathbf{U}}^n_i\right)_\alpha}{(\widehat{\mathbf{U}}^n_i)_\alpha}} \leq 1 \text{ gives } \boxed{\frac{(\mathbb{A}_i\mathbf{U}^n_i)_\alpha}{(\mathbf{U}^n_i)_\alpha} \geq \left|\frac{(\mathbb{A}_{i+1}\mathbf{U}^n_i)_\alpha}{(\mathbf{U}^n_i)_\alpha} + \frac{(\mathbb{A}_{i-1}\mathbf{U}^n_i)_\alpha}{(\mathbf{U}^n_i)_\alpha}\right|}$$

Analysis of multi-D Euler equations linearization procedure

Stability analysis

Generic implicit structure:

$$\left(\frac{\mathbb{I}}{\Delta t}+\sum_f S_f \mathbb{A}_{cf}\right)\Delta \mathbf{U}_c-\sum_f S_f \mathbb{A}_{df}\Delta \mathbf{U}_d=\sum_f S_f \Phi_f^n(\mathbf{n}_{cf})$$

1D stability criterion:

$$\frac{(\mathbb{A}_i \mathbf{U}_i^n)_\alpha}{(\mathbf{U}_i^n)_\alpha} \geq \left|\frac{(\mathbb{A}_{i+1} \mathbf{U}_i^n)_\alpha}{(\mathbf{U}_i^n)_\alpha}+\frac{(\mathbb{A}_{i-1} \mathbf{U}_i^n)_\alpha}{(\mathbf{U}_i^n)_\alpha}\right|$$

We extend the 1D stability criterion to Multi-D: $\boxed{\sum_f S_f \frac{(\mathbb{A}_{cf}\mathbf{U}_c)_\alpha}{(\mathbf{U}_c)_\alpha} \geq \left|\sum_f S_f \frac{(\mathbb{A}_{df}\mathbf{U}_c)_\alpha}{(\mathbf{U}_c)_\alpha}\right|}$

Classic [8] lin.: $\Delta\Phi_f \approx \frac{\mathbb{J}_c^n \Delta\mathbf{U}_c + \mathbb{J}_d^n \Delta\mathbf{U}_d}{2} - |\mathbb{J}_f^n| \frac{\Delta\mathbf{U}_d - \Delta\mathbf{U}_c}{2}$ $\quad \mathbb{A}_{cf}=\frac{|\mathbb{J}_f| - \mathbb{J}_c}{2}$ & $\mathbb{A}_{df}=\frac{|\mathbb{J}_f| - \mathbb{J}_d}{2}$

Using $\Delta\mathbf{F}_c \approx \mathbb{J}_c^n \Delta\mathbf{U}_c$

Monotone [4] lin.: $\Delta\Phi_f \approx \frac{\Delta\mathbf{F}_c + \Delta\mathbf{F}_d}{2} - |\mathbb{J}_f^n| \frac{\Delta\mathbf{U}_d - \Delta\mathbf{U}_c}{2}$ $\quad \mathbb{A}_{cf}=\mathbb{A}_{df}=\frac{|\mathbb{J}_f| - \mathbb{J}_f}{2}$

Using: $\sum_f S_f \mathbf{F}_c \mathbf{n}_{cf} = 0$ & $\Delta\mathbf{F}_d - \Delta\mathbf{F}_c \approx \mathbb{J}_f^n(\Delta\mathbf{U}_d - \Delta\mathbf{U}_c)$

Classic: condition not respected

Monotone: condition respected

Analysis of multi-D Euler equations linearization procedure

Numerical results

1D stationary shock wave:

- Mach 20, $\gamma = 1.4$
- 50 cells uniform mesh over [0; 1] domain

Variable	Left BC	Right BC	Unity
ρ	0.741	0.125	$[kg.m^{-3}]$
u	-11.30	-66.93	$[m.s^{-1}]$
p	466.5	1.0	$[Pa]$

Initial Conditions from Rankine-Hugoniot relations

Classic vs monotone: comparison **Initial & final density**

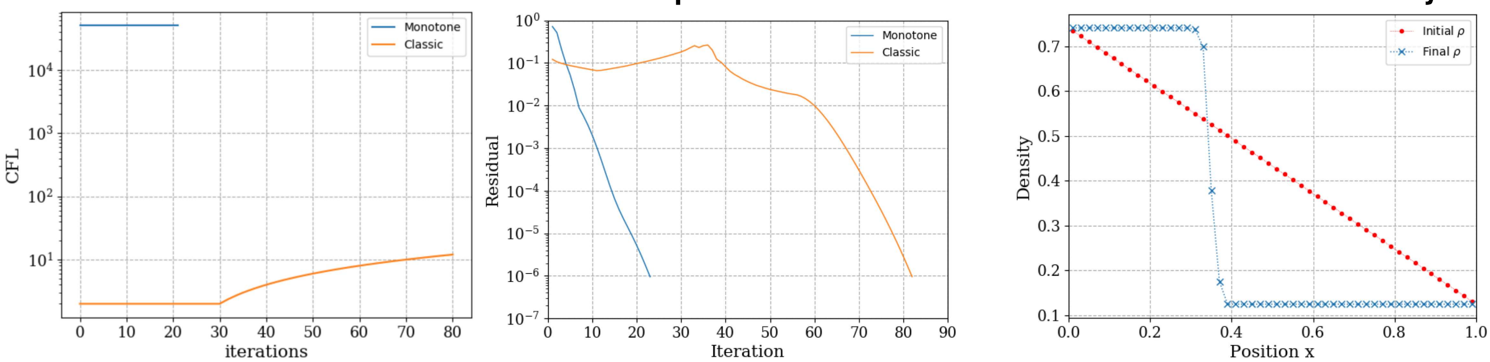

- Monotone linearization procedure respects stability criterion & is more robust.

Numerical results

M20 stationary shock around half cylinder

- Mach 20, $\gamma = 1.4$
- 5000 quadrangles mesh

Variable	Initial state	Unity
ρ	1.0	$[\mathrm{kg.m^{-3}}]$
u_x	23.66	$[\mathrm{m.s^{-1}}]$
u_y	0.0	$[\mathrm{m.s^{-1}}]$
p	1.0	$[\mathrm{Pa}]$

Table: Initial Conditions

Classic vs monotone: comparison

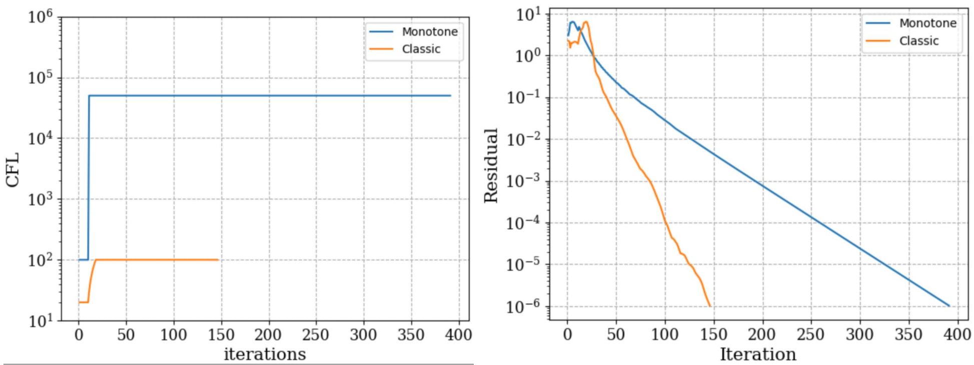

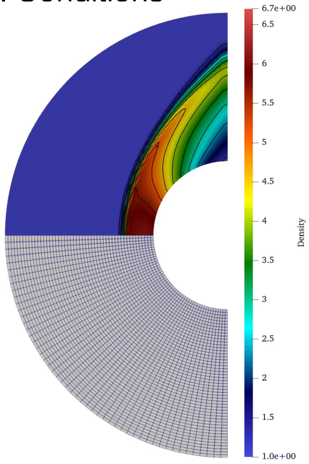

Map & contour of density

- Monotone linearization procedure more robust & classic linearization procedure converges faster

Analysis of multi-D Euler equations linearization procedure

Numerical results

M20 stationary shock around half cylinder

- Mach 20, $\gamma = 1.4$
- 6971 triangles mesh

Variable	Initial state	Unity
ρ	1.0	$[\mathrm{kg.m}^{-3}]$
u_x	23.66	$[\mathrm{m.s}^{-1}]$
u_y	0.0	$[\mathrm{m.s}^{-1}]$
p	1.0	$[\mathrm{Pa}]$

Table: Initial Conditions

Classic vs monotone: comparison

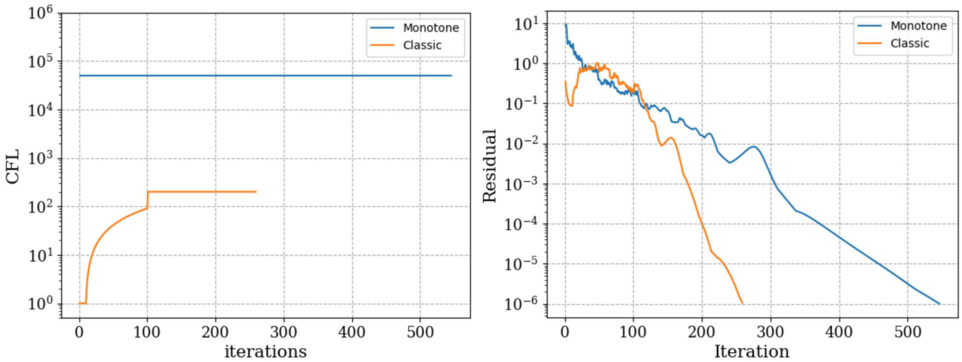

- Monotone linearization procedure more robust & classic linearization procedure converges faster

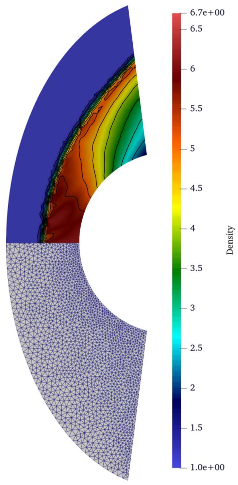

Map & contour of density

-

Analysis of multi-D Euler equations linearization procedure

Numerical results

Mach 3 backward facing step

- Mach 3, $\gamma = 1.4$
- 9724 triangular mesh

Variable	Initial state	Inlet state	Unity
ρ	1.0	3.90	$[\mathrm{kg.m}^{-3}]$
u_x	0.0	2.22	$[\mathrm{m.s}^{-1}]$
u_y	0.0	0.0	$[\mathrm{m.s}^{-1}]$
p	1.0	7.38	[Pa]

Table: Initial Conditions

Classic vs monotone: comparison

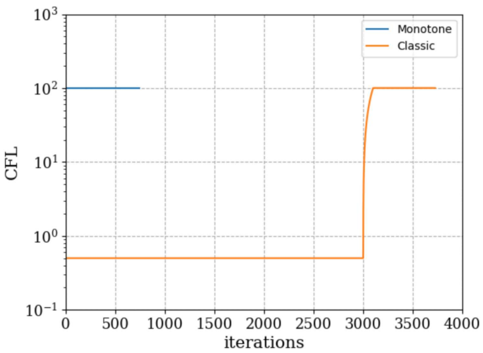

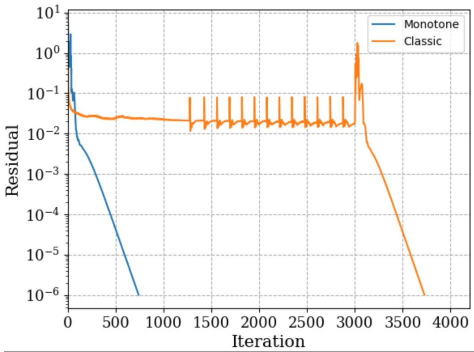

- Classic linearization procedure diverges for any attempt of increasing explicit CFL before 3000 iterations!

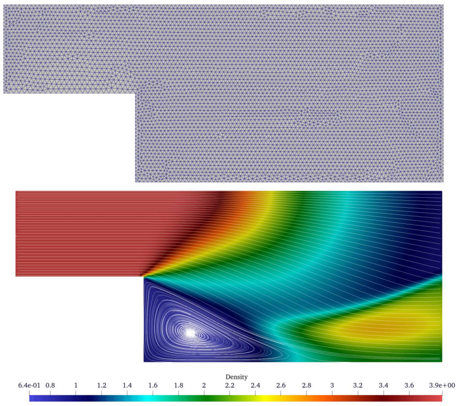

Map of density & streamlines

Linear stability analysis

Generic linearization for implicit schemes

We recast any $\Phi^n_{i+1/2}$ into a classical finite volume flux:

$$\Phi^n_{i+1/2} = \frac{\mathbf{F}^n_{i+1} + \mathbf{F}^n_i}{2} - \mathbb{B}_{i+1/2}\frac{\mathbf{U}^n_{i+1} - \mathbf{U}^n_i}{2}$$

Assumption: $\mathbb{B}_{i+1/2}$ has the same eigenvectors as $\mathbb{J}_{i+1/2}$, $\quad \mathbb{J}_{i+1/2} = \mathbb{R}_{i+1/2}\,(\text{diag}(\lambda_k))_{i+1/2}\,\mathbb{L}_{i+1/2}$

$$\mathbb{B}_{i+1/2} = \mathbb{R}_{i+1/2}\begin{pmatrix} b_{1,i+1/2} & 0 & 0 \\ 0 & b_{2,i+1/2} & 0 \\ 0 & 0 & b_{3,i+1/2} \end{pmatrix}\mathbb{L}_{i+1/2}, \qquad \mathbb{B}_{i+1/2} = \mathbb{R}_{i+1/2}\,(\text{diag}(b_k))_{i+1/2}\,\mathbb{L}_{i+1/2}$$

The b_k are computed using:

$$b_{k,i+1/2} = \frac{\left(\mathbb{L}_{i+1/2}((\mathbf{F}^n_{i+1} + \mathbf{F}^n_i) - 2\Phi^n_{i+1/2})\right)_k}{\left(\mathbb{L}_{i+1/2}(\mathbf{U}^n_{i+1} - \mathbf{U}^n_i)\right)_k}$$

The 1D implicit scheme writes:

$$\frac{\Delta\mathbf{U}_i}{\tau} + \underbrace{\frac{\mathbf{F}^{n+1}_{i+1} - \mathbf{F}^{n+1}_{i-1}}{2}}_{\text{Convective term}} = \underbrace{\mathbb{B}_{i+1/2}\frac{\mathbf{U}^n_{i+1} - \mathbf{U}^n_i}{2} - \mathbb{B}_{i-1/2}\frac{\mathbf{U}^n_i - \mathbf{U}^n_{i-1}}{2} + |\mathbb{J}^n_{i+1/2}|\frac{\Delta\mathbf{U}_{i+1} - \Delta\mathbf{U}_i}{2} - |\mathbb{J}^n_{i-1/2}|\frac{\Delta\mathbf{U}_i - \Delta\mathbf{U}_{i-1}}{2}}_{\text{Diffusion terms}}$$

Linear stability analysis

A novel matrix correction

The convective term in the eigen space is linearly unconditionally stable using a criterion from v. Neumann analysis

Analysis of the diffusive term in the eigen space:

$$\boxed{\begin{aligned}\frac{(\mathbb{L}_i \Delta \mathbf{U}_i)_k}{\tau} &= b_{i+1/2,k}\frac{(\mathbb{L}_i(\mathbf{U}^n_{i+1}-\mathbf{U}^n_i))_k}{2} &&- b_{i-1/2,k}\frac{(\mathbb{L}_i(\mathbf{U}^n_i-\mathbf{U}^n_{i-1}))_k}{2}\\ &+ |\lambda^n_{i+1/2,k}|\frac{(\mathbb{L}_i(\Delta\mathbf{U}_{i+1}-\Delta\mathbf{U}_i))_k}{2} &&- |\lambda^n_{i-1/2,k}|\frac{(\mathbb{L}_i(\Delta\mathbf{U}_i-\Delta\mathbf{U}_{i-1}))_k}{2}\end{aligned}}$$

With: $\begin{aligned}\mathbb{L}_i|\mathbb{J}_{i\pm1/2}| &= (\text{diag}(|\lambda_{i,k}|))\,\mathbb{L}_i\\ \mathbb{L}_i\mathbb{B}_{i\pm1/2} &= (\text{diag}(b_{i,k}\ \ ))\,\mathbb{L}_i\end{aligned}$ & $(\text{w}_j)_k = (\mathbb{L}_i\mathbf{U}_j)_k$ for $j = i-1, i, i+1$

v. Neumann analysis gives criterion $\boxed{2|\lambda_{i,k}| \geq b_{i,k} \geq 0}$ to ensure linear stability

Matrix correction:

$$\boxed{\text{if } |\lambda_{i,k}| < b_{i,k}, \text{ then} |\tilde{\lambda_{i,k}}| = |\lambda_{i,k}| + c_{i+1/2}}$$

Linear stability analysis

Numerical results

1D stationary shock wave:

- Mach 20, $\gamma = 1.4$
- 50 cells uniform mesh over [0; 1] domain
- $\frac{||\mathbf{U}^{n+1} - \mathbf{U}^n||_1}{||\mathbf{U}^0||_1} \leq 10^{-6}$ as convergence criterion

Variable	Left BC	Right BC	Unity
ρ	0.741	0.125	$[\mathrm{kg.m}^{-3}]$
u	-11.30	-66.93	$[\mathrm{m.s}^{-1}]$
p	466.5	1.0	$[\mathrm{Pa}]$

ICs from Rankine-Hugoniot relations

Initial & final density

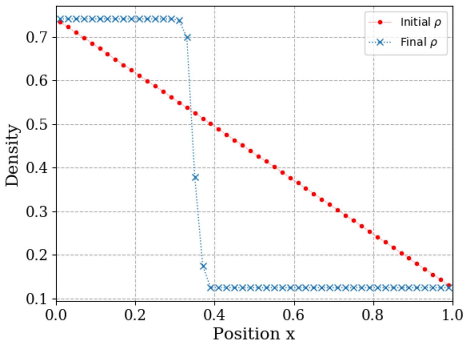

Non-corrected vs corrected: comparison

RHS Scheme	Max CFL	
	no correction	correction
FV-Roe [6]	50 000	50 000
SLAU [2]	50 000	50 000
HLLE [3]	10	50 000
Rusanov [7]	2	50 000

- No correction needed for SLAU or FV-Roe.
- Correction added with HLLE or Rusanov strongly increases robustness.

Linear stability analysis

Numerical results

M20 stationary shock around half cylinder

- Mach 20, $\gamma = 1.4$
- 5000 quadrangles mesh

Variable	Initial state	Unity
ρ	1.0	$[\mathrm{kg.m}^{-3}]$
u_x	23.66	$[\mathrm{m.s}^{-1}]$
u_y	0.0	$[\mathrm{m.s}^{-1}]$
p	1.0	$[\mathrm{Pa}]$

Table: Initial Conditions

Non-corrected vs corrected: comparison

RHS Scheme	Max CFL	
	no correction	correction
FV-Roe [6]	100	100
SLAU [2]	300	50 000
HLLE [3]	5	50 000
Rusanov [7]	5	50 000

- Correction added with HLLE, Rusanov or SLAU strongly increases robustness

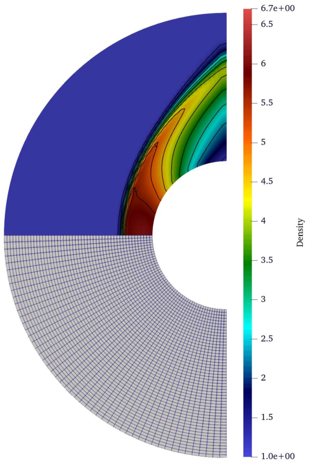

Map & contour of density

Linear stability analysis

Numerical results

M20 stationary shock around half cylinder

- Mach 20, $\gamma = 1.4$
- 5000 quadrangles mesh

Variable	Initial state	Unity
ρ	1.0	$[\mathrm{kg.m^{-3}}]$
u_x	23.66	$[\mathrm{m.s^{-1}}]$
u_y	0.0	$[\mathrm{m.s^{-1}}]$
p	1.0	$[\mathrm{Pa}]$

Table: Initial Conditions

Non-corrected vs corrected: comparison

RHS Scheme	Max CFL	
	no correction	correction
FV-Roe [6]	50 000	50 000
SLAU [2]	50	500
HLLE [3]	5	10
Rusanov [7]	5	200

- Correction added with HLLE, Rusanov or SLAU increases robustness

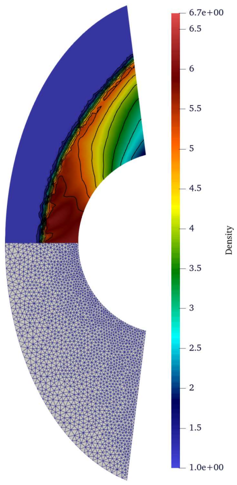

Map & contour of density

Linear stability analysis

Numerical results

M20 stationary shock around cylinder

- Mach 20, $\gamma = 1.4$
- 9702 quadrangles mesh
- Same initial conditions as half-cylinder

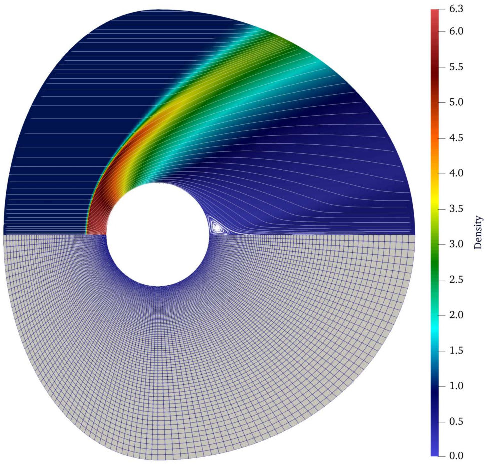

Mesh, Map of density & streamlines

Non-corrected vs corrected: comparison

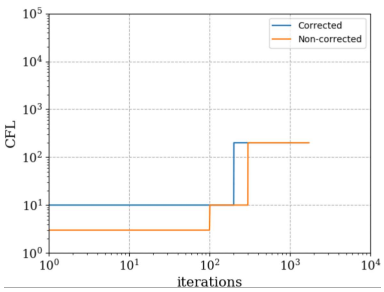

SLAU [2]

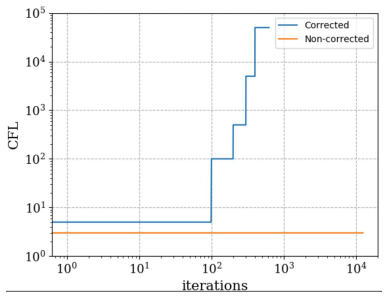

Rusanov [7]

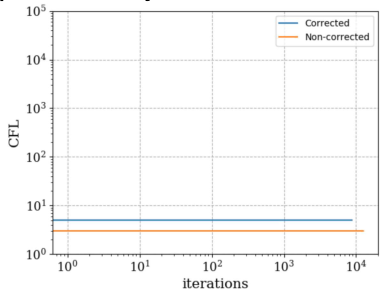

HLLE [3]

Linear stability analysis

Numerical results

M20 stationary shock around cylinder

- Mach 20, $\gamma = 1.4$
- 9844 triangles mesh
- Same initial conditions as half-cylinder

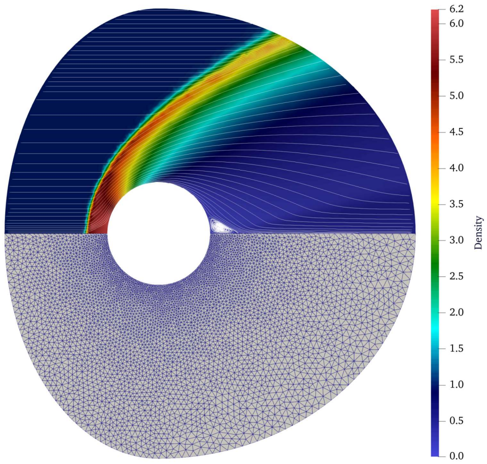

Mesh, Map of density & streamlines

Non-corrected vs corrected: comparison

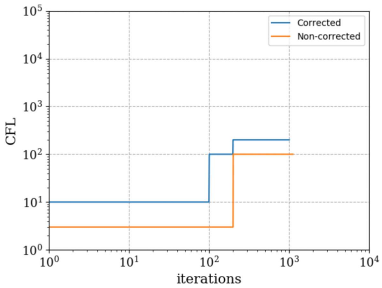

SLAU [2]

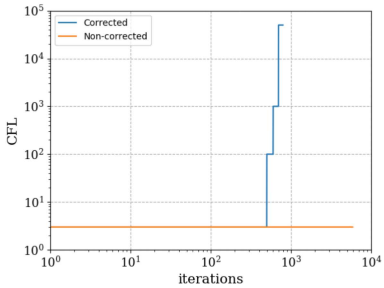

Rusanov [7]

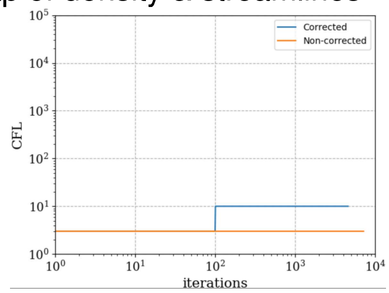

HLLE [3]

-

A new paradigm: flux re-formulation of Euler equations

Discretized model:

$$\frac{\mathbf{U}_c^{n+1} - \mathbf{U}_c^n}{\Delta t} + \sum_f S_f \Phi_f^{n+1}.\mathbf{n}_{cf} = 0$$

$\Rightarrow$ $\boxed{\times \mathbb{J}_c^n(\mathbf{p}_c)}$ $\Rightarrow$

$\Delta \mathbf{F}_c(\mathbf{p}_c) \approx \mathbb{J}_c^n(\mathbf{p}_c)\Delta \mathbf{U}_c$

Discretized model:

$$\frac{\mathbf{F}_c^{n+1}(\mathbf{p}_c) - \mathbf{F}_c^n(\mathbf{p}_c)}{\Delta t} + \mathbb{J}_c^n(\mathbf{p}_c) \sum_f S_f \Phi_f^{n+1}.\mathbf{n}_{cf} = 0$$

$\Rightarrow$ To limit the effect of the strong non-linearity between **U** and **F** on the solving of the linear system.
$\Rightarrow$ To chose a direction of resolution.

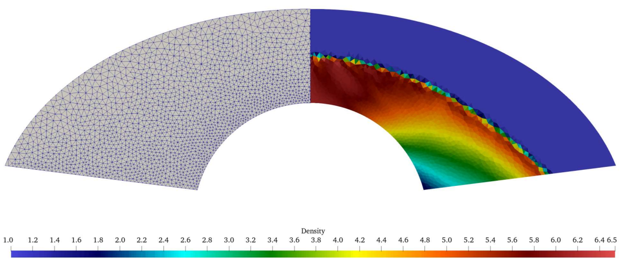

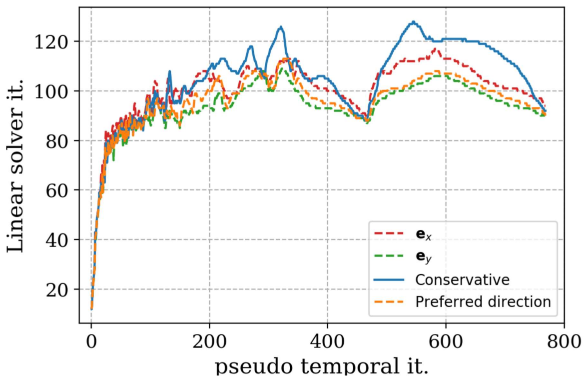

Conclusion & outlook

- We proposed a theoretical tool to analyse implicit linear schemes and build novels ones.
- We have shown its relevance comparing two implicit linearization procedures, a classical one [8] and a monotone one [4] over several test cases.
- We proposed to adapt Roe based matrix to arbitrary RHS scheme using matrix correction based on a stability linear analysis.
- We tried a new linearization procedure based on flux reformulation of Euler equations.
- **Futur work:** Extension of this work to 2nd order space accuracy.
- **Outlook:** extend this work to 3D Navier-Stokes equations & challenging it over several industrial test cases and find new linearization procedures to better precondition the linear system.
- **Communication:**
  "Toward robust linear implicit schemes for steady state hypersonic flows", submitted on april, JCP.
  "Novels linear implicit schemes based on flux reformulation of Euler equations", in preparation.

References I

[1] Agnes Chan. “Innovative numerical schemes for 3D supersonic aerodynamics on unstructured mesh.”. PhD thesis. Université de Bordeaux, 2022.

[2] Keiichi Kitamura Eiji Shima. “Parameter-Free Simple Low-Dissipation AUSM-Family Scheme for All Speeds”. In: *American Institute of Aeronautics and Astronautics* 49.8 (2011), pp. 1693–1709. DOI: 10.2514/1.J050905. URL: https://arc.aiaa.org/doi/10.2514/1.J050905.

[3] Bernd Einfeldt. “On Godunov-Type Methods for Gas Dynamics”. In: *SIAM Journal on Numerical Analysis* 25.2 (1988), pp. 294–318. DOI: 10.1137/0725021. eprint: https://doi.org/10.1137/0725021. URL: https://doi.org/10.1137/0725021.

[4] R. F. Warming H. C. Yee and A. Harten. “Implicit Total Variation Diminishing (TVD) Schemes for Steady-State Calculations”. In: *Journal of Computational Physics* 57 (1985), pp. 327–360.

References II

[5] A. Harten. “High Resolution Schemes for Hyperbolic Conservation Laws”. In: *Journal of Computational Physics* 135 (1997), 260–278.

[6] Jean Marie Masella, Isabelle Faille, and Thierry Gallouët. “On a rough Godunov scheme”. In: *Comptes Rendus Académie des Sciences de Paris* I-323 (1996), 77–84.

[7] V.V. Rusanov. *Calculation of Interaction of Non-steady Shock Waves with Obstacles*. Technical translation. National Research Council of Canada, 1962. URL: https://books.google.fr/books?id=9Tq5SgAACAAJ.

[8] H.C. Yee. “A class of high-resolution explicit and implicit shock capturing methods”. In: *CFD, Lecture Series, Von Karman Institute fo Fluid Dynamics* (1989).